# Supporting Information

## Voltage-Driven Engineering for Concurrent Enhancement of Ferroelectricity and Endurance in HZO-Based Ferroelectric Devices

**Author names**

*Wonwoo Kho[a], Hyunjoo Hwang[a], Hyunjun Kim[b], Dongjun Min[b], Narim Lee[b], and Seung-Eon Ahn*[a,b]*

**Author address**

[a]Department of IT · Semiconductor Convergence Engineering, Tech University of Korea, Siheung 15073, Republic of Korea

[b]Department of Semiconductor Engineering, Tech University of Korea, Siheung 15073, Republic of Korea

E-mail: seahn@tukorea.ac.kr

Keywords: HZO, ferroelectric, cycling effect, endurance, domain de-pinning.

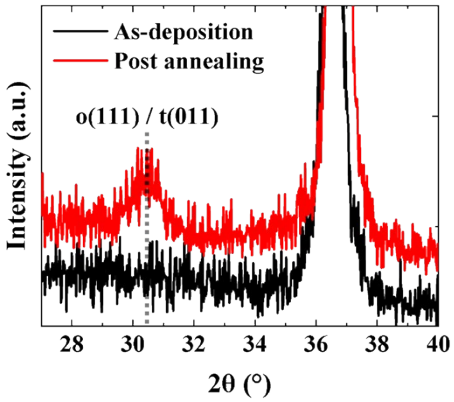


**Fig. S1** GI-XRD data before and after crystallisation.

Following crystallization, diffraction peaks corresponding to o(111) and/or t(011) were observed. Because the o(111) and t(011) reflections lie in close proximity, it is challenging to attribute these peaks exclusively to the ferroelectric o-phase. Therefore, the most direct and reliable evidence of ferroelectricity or antiferroelectricity is obtained from transient switching currents and the resulting P–V hysteresis characteristics, which arise from switchable polarization under an applied electric field.

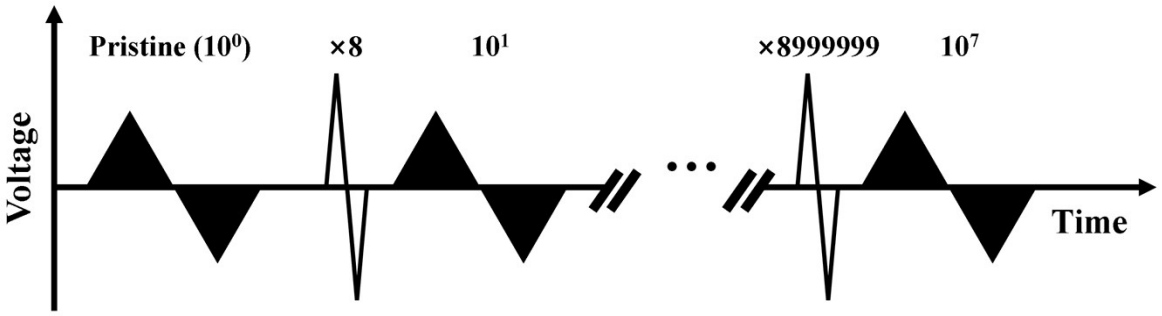


**Fig. S2** Measurement sequence for extracting pulsed J–V curves under various cycling voltage conditions.

Pulsed J–V curves were acquired by applying ±1.5 V triangular pulses at 1 kHz, with a fixed pulse width of 5 μs. Cycling was performed by repeatedly applying pulses at each target voltage amplitude. Pulsed J–V curves were extracted and analysed at specific intervals: cycles $10^0$ (pristine), $10^1$, ..., up to $10^7$.

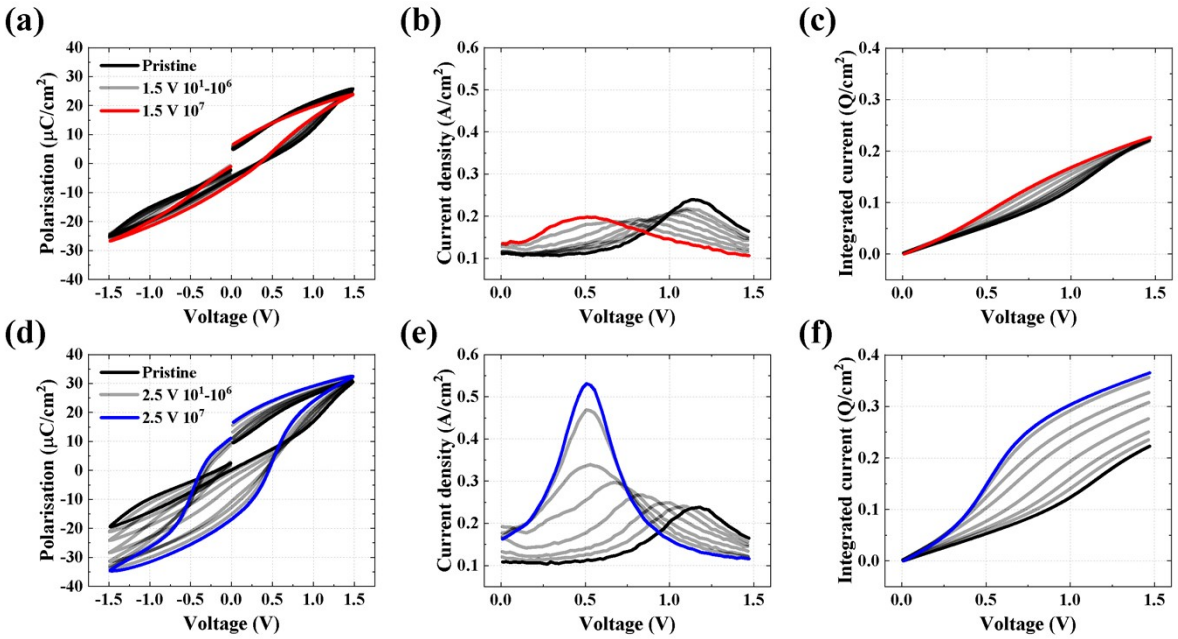


**Fig. S3** P–V curves obtained under various voltage cycling conditions, and transient currents of the first quadrant of the pulsed J–V curve. P–V curves obtained by integrating the transient current of pulsed J–V curves during (a) ±1.5 V and (d) ±2.5 V cycling up to $10^7$ cycles. Transient current components induced during the rising edge of the applied positive triangular pulse for (b) ±1.5 V and (e) ±2.5 V cycling. Corresponding integrated values of transient current from the first quadrant of the pulsed J–V curve for (c) ±1.5 V and (f) ±2.5 V cycling.

During pulsed J–V measurements, the transient current induced during the rising edge of the applied positive triangular pulse—corresponding to the first quadrant of the pulsed J–V curve—reflects only the polarisation switching of the ferroelectric phase and the first switching event of the antiferroelectric phase. By integrating this region, the contribution from the second polarisation reversal of the antiferroelectric component is excluded. Thus, this approach provides a quantitative measure of polarisation induced solely by switching events, allowing total polarisation switching response analysis of ferroelectric and antiferroelectric.

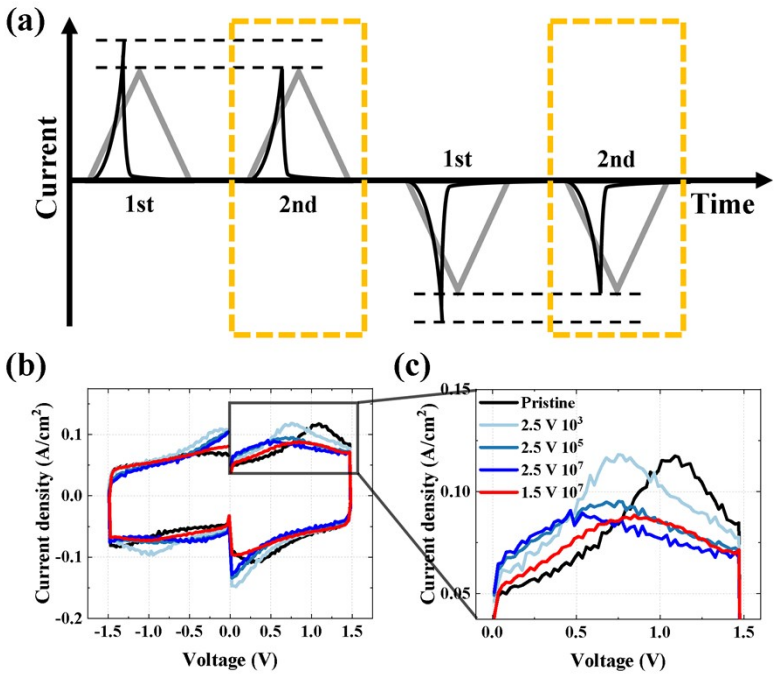


**Fig. S4** Non-ferroelectric component analysis. (a) Measurement sequence for extracting pulsed J–V curves excluding transient currents from ferroelectric switching. (b) Pulsed J–V curves obtained from the second triangle pulse in the sequence. (c) Magnified view of transient currents during the rising edge of the positive pulse in the first quadrant.

By analysing the non-ferroelectric component, the transient current associated with antiferroelectricity—excluding that from ferroelectric switching—can be evaluated. To this end, we extracted the pulsed J–V curves from the second triangle pulse, which does not involve ferroelectric polarisation switching, to assess the antiferroelectric response originating from the t-phase. If the t-to-o phase transition were the primary mechanism of the wake-up effect, a large transient current should be observed in the pristine state due to antiferroelectricity, and this current should significantly decrease after ±2.5 V cycling, where $P_r$ increases markedly. However, the transient current after ±2.5 V cycling remained nearly identical to that after ±1.5 V cycling. These results strongly suggest that the observed $P_r$ increase in ±2.5 V cycling is unlikely to stem from a phase transition.

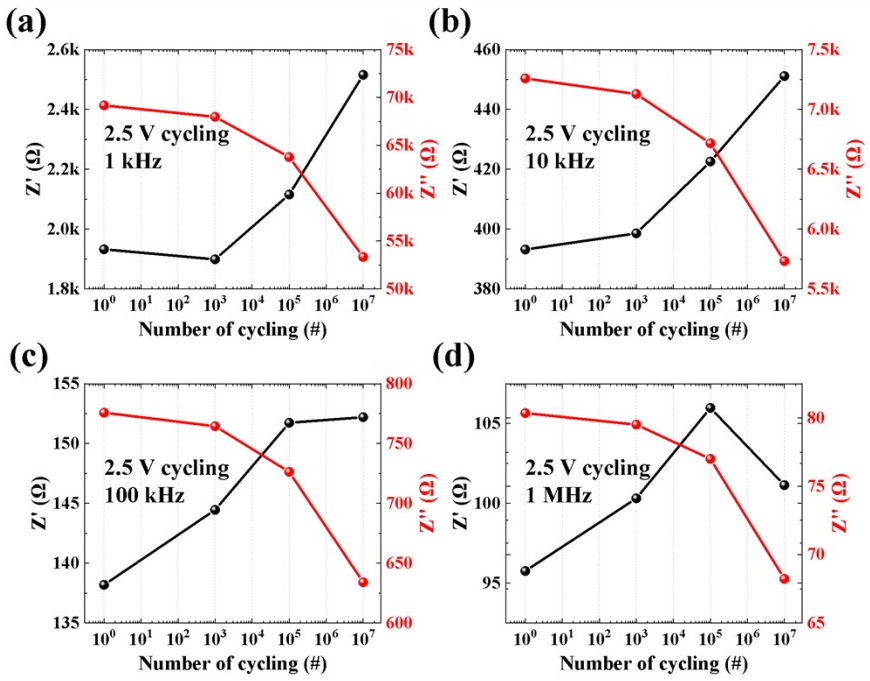


**Fig. S5** Impedance response after pristine and ±2.5 V cycling at $10^3$, $10^5$, and $10^7$ cycles. Impedance response obtained at (a) 1 kHz, (b) 10 kHz, (c) 100 kHz, and (d) 1 MHz.

The Z′ value generally increased with cycling; however, a reduction was observed at high frequencies and after extensive cycling. In contrast, the Z″ value decreased with cycling, exhibiting a similar trend across all frequencies.

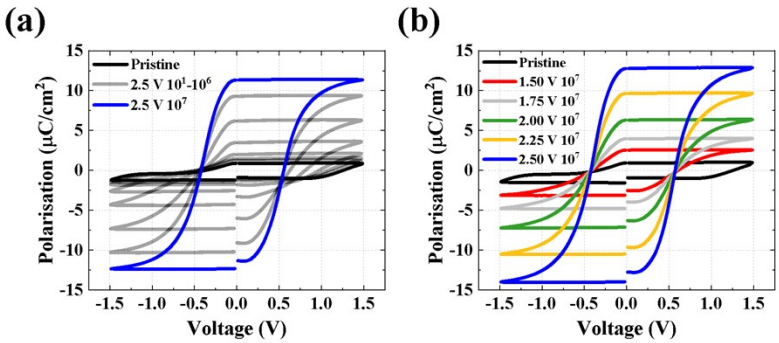


**Fig. S6** P–V curves from PUND measurements under two different cycling methods. (a) P–V curve obtained by integrating the transient current after pristine and ±2.5 V cycling at $10^3$, $10^5$, and $10^7$ cycles. (b) P–V curve obtained by integrating the transient current after $10^7$ cycles at each increment from ±1.5 V to ±2.5 V (ΔV = ±0.25 V) using the append method.

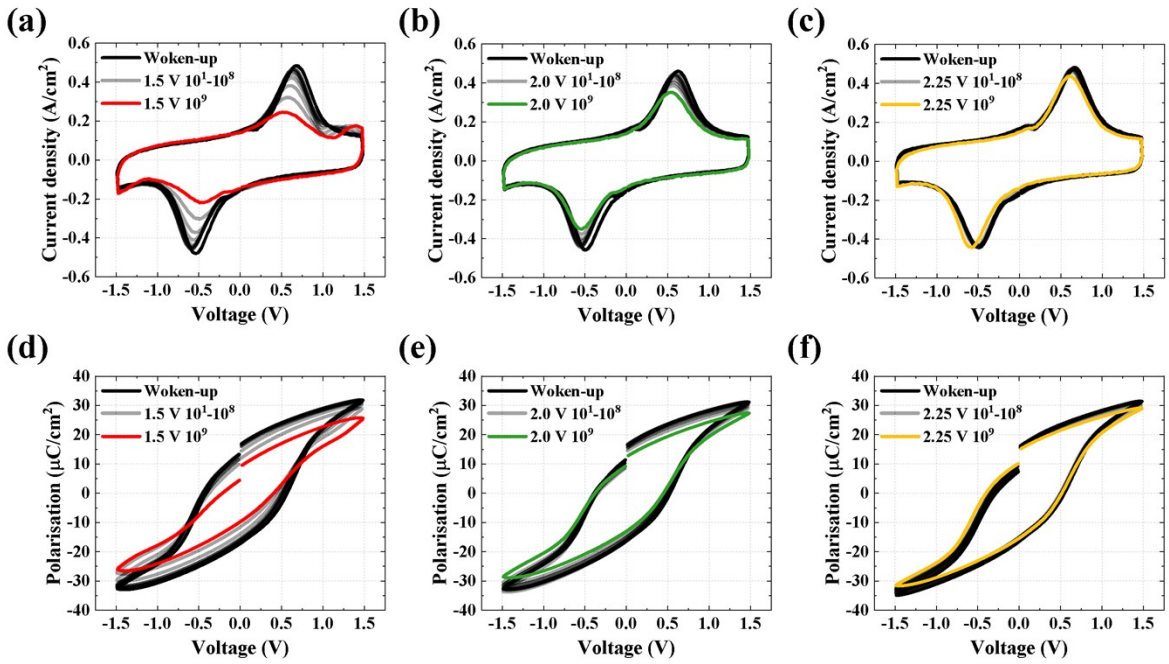


**Fig. S7** Endurance characteristics under different operating ranges. Pulsed J–V curves obtained during endurance cycling up to $10^9$ cycles for operating ranges of (a) ±1.5 V, (b) ±2.0 V, and (c) ±2.25 V. Corresponding P–V curves obtained by integrating the transient current for operating ranges of (d) ±1.5 V, (e) ±2.0 V, and (f) ±2.25 V.